

# The Effect of Additional Elements and Grain Size Distribution on the Magnetic Properties of the Nd-Fe-B Sintered Magnets

Y. G. Hong and C. O. Kim

Department of Materials Engineering, Chung-Nam National University, Taejon 305-764, Korea

Nd-Fe-B계 소결자석의 자기적 특성에 미치는 첨가원소와 결정립 분포의 영향

홍연기·김종오

충남대학교 공과대학 재료공학과

(1998년 4월 20일 받음, 1998년 7월 9일 최종수정본 받음)

**초 록** 합금의 주조시 냉각속도가 Nd<sub>16</sub>Fe<sub>72</sub>V<sub>4</sub>B<sub>8</sub> 소결자석의 결정립 분포와 착자특성에 미치는 영향에 대하여 조사하였다. 냉각속도가 높은 Cu mold를 사용하여 제작한 시료는 좁은 결정립 분포와 착자특성의 향상을 보였다. B화합물을 생성하는 Cr, Mn, Nb 그리고 W과 같은 첨가원소가 Nd-Fe-B계 소결자석의 착자특성에 미치는 영향에 대해서도 조사하였다. Cr이나 W첨가는 보자력의 향상에 효과적이고 Nd<sub>16</sub>Fe<sub>72</sub>Cr<sub>4</sub>B<sub>8</sub>합금은 Nd<sub>16</sub>Fe<sub>72</sub>V<sub>4</sub>B<sub>8</sub>합금과 비슷한 착자특성을 보였다.

**Abstract** The influence of casting cooling rate during the preparation of ingots on the grain size distribution and the magnetizing ability of Nd<sub>16</sub>Fe<sub>72</sub>V<sub>4</sub>B<sub>8</sub> sintered magnets were investigated. Sintered magnets prepared from copper mold, which allow a higher cooling rate, show a smaller grain size distribution and good magnetizing ability. The effects of adding boride forming elements, such as Cr, Mn, Nb, and W on the magnetic properties of Nd-Fe-B sintered magnets were also investigated. Both Cr and W addition increase coercivity and the resultant Nd<sub>16</sub>Fe<sub>72</sub>Cr<sub>4</sub>B<sub>8</sub> alloy exhibits a similar magnetizing ability in comparison with Nd<sub>16</sub>Fe<sub>72</sub>V<sub>4</sub>B<sub>8</sub> alloy.

## 1. Introduction

Since development of the first Nd-Fe-B permanent magnet much research has been done in this new field.<sup>1-4)</sup> Practical applications of these magnets have been made in various fields including telecommunications, data processing, acoustic transducers, and motor technologies.

In order to produce high performance Nd-Fe-B sintered magnets the alloy composition must be close to the stoichiometric relationship of Nd<sub>2</sub>Fe<sub>14</sub>B.<sup>5)</sup> This helps in reducing loss of coercivity and enhances alignment of the Nd<sub>2</sub>Fe<sub>14</sub>B grains in the alloy. Improvements in thermal stability and corrosion resistance have also been required in order to expand useful applications of these magnets. Dysprosium is one essential element in improving thermal stability because it significantly increases magnetic anisotropy of the Nd<sub>2</sub>Fe<sub>14</sub>B main phase.<sup>7)</sup> Cobalt is another essential element in improving the temperature coefficient of the remanence (B<sub>r</sub>) through a significant increase in the Curie temperature.<sup>6)</sup> Cobalt has the added benefit of stabilizing the Nd-

rich phase against oxidation and contributing to improved corrosion resistance.<sup>8)</sup> However the high material cost of Dy and a reduction of the intrinsic coercivity due to Co addition are disadvantages of using these elements as additives.

Sagawa et al.<sup>6)</sup> and Hirosawa et al.<sup>8)</sup> have shown that addition of either V or Mo is effective for improving the thermal stability and corrosion resistance of Nd-(Dy)-Fe-Co-B sintered magnets, which also exhibit high magnetizing ability.<sup>10)</sup> Addition of these two elements acts to form V<sub>3-x</sub>Fe<sub>x</sub>B<sub>2</sub> or Mo<sub>2</sub>FeB<sub>2</sub><sup>8)</sup> borides in the metallic alloy of the magnets. These borides inhibit grain size growth during sintering, resulting in a smaller average grain size.<sup>9)</sup> The strength of the local demagnetization field decreases with smaller grain size leading to an improvement in the magnetizing ability of V or Mo added Nd-Fe-B sintered magnets. This study investigates the influence of the cooling rate of casting on grain size distribution in V containing Nd-Fe-B sintered magnets and investigates the effect of additional elements (Cr, Mn, Nb, and W) on the magnetic properties and the grain size

distribution of Nd-Fe-B sintered magnets.

## 2. Experimental Procedures

$\text{Nd}_{16}\text{Fe}_{72}\text{M}_4\text{B}_8$  alloys ( $M = \text{V}, \text{Cr}, \text{Mn}, \text{Nb}$  and  $\text{W}$ ) were induction-melted under an Ar atmosphere and cast in  $50\text{mm} \times 5\text{mm} \times 100\text{mm}$  molds. Either copper or iron molds were used in order to better control the casting cooling rate. The alloys were crushed into a coarse powder ( $63\mu\text{m} \sim 500\mu\text{m}$ ), then ball-milled to a fine powder of  $2.5\mu\text{m}$  in diameter. Powders were aligned in a magnetic field of  $0.96 \text{ MA/m}$  and pressed in a direction perpendicular to the grain alignment. The resulting green compacts were sintered first in a vacuum, then under an Ar atmosphere at temperatures between  $1333\text{K}$  and  $1393\text{K}$ , followed by controlled-cooling to room temperature at a rate of  $50\text{K/h}$ . Magnetic properties of sintered magnets were measured using a B-H loop tracer.

Kanekiyo et al. measured magnetizing ability by the extraction method. Estimations were based on the value of the effective magnetizing field ( $H_{\text{eff}}$ ). The  $H_{\text{eff}}$  is defined as :

$$H_{\text{eff}} = H_A - H_d$$

where  $H_A$  represents the applied field where 90% magnetization is obtained and  $H_d$  represents the demagnetizing field.<sup>10)</sup>

In this study, Magnetizing ability was measured by V. S. M. Estimations were based on the dependence of relative magnetic properties on the applied field. Samples for measurement of magnetizing abilities were prepared by cutting the sintered compacts into a cube of  $2.5\text{mm} \times 2.5\text{mm} \times 2.5\text{mm}$ . Relative magnetic properties were normalized using the ratio of magnetic properties in the applied magnetizing field to magnetic properties after ap-

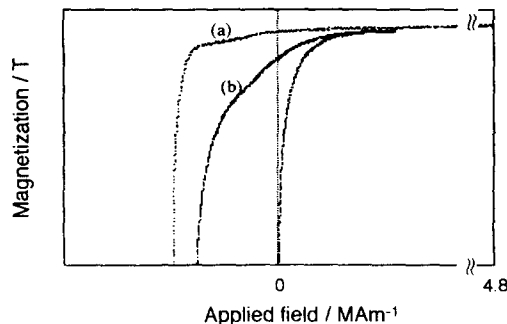


Fig. 1. Estimation of magnetizing ability. (a) applied  $4.8\text{MAm}^{-1}$ , and (b) lower than  $4.8\text{MAm}^{-1}$ .

plying a pulsed field of  $4.8\text{MA/m}$  as in figure 1. The microstructure was observed using optical microscope. The average grain size and the grain size distribution were calculated from optical micrographs.

## 3. Results and Discussion

Figure 2 shows optical micrographs of  $\text{Nd}_{16}\text{Fe}_{72}\text{V}_4\text{B}_8$  ingots prepared from copper and iron molds. The grain size from copper mold is smaller than from iron mold because the cooling rate of casting with copper is higher. Figure 3 shows variations of the magnetic properties of  $\text{Nd}_{16}\text{Fe}_{72}\text{V}_4\text{B}_8$  sintered magnets due to copper and iron molds vs. sintering temperatures in comparison with  $\text{Nd}_{16}\text{Fe}_{76}\text{B}_8$  magnets. The density of the samples is slightly increased with increasing sintering temperatures. Remanence and  $(\text{BH})_{\text{max}}$  values are also gradually increased with increasing sintering temperatures, with a maximum value at  $1373\text{K}$ . Coercivity decreases with increasing temperatures. The remanence and  $(\text{BH})_{\text{max}}$  values of  $\text{Nd}_{16}\text{Fe}_{72}\text{V}_4\text{B}_8$  sintered magnets are both lower than for  $\text{Nd}_{16}\text{Fe}_{76}\text{B}_8$  magnets, but the coercivity of  $\text{Nd}_{16}\text{Fe}_{72}\text{V}_4\text{B}_8$  sintered magnets is higher.  $\text{Nd}_{16}\text{Fe}_{72}\text{V}_4\text{B}_8$  sintered magnets prepared from copper mold show higher remanence and  $(\text{BH})_{\text{max}}$  values than magnets prepared from iron mold. Figure 4 shows a dependence of relative  $(\text{BH})_{\text{max}}$ , relative  $B_r$ , and relative coercivity values on the applied magnetic field for  $\text{Nd}_{16}\text{Fe}_{76-x}\text{V}_x\text{B}_8$  (X

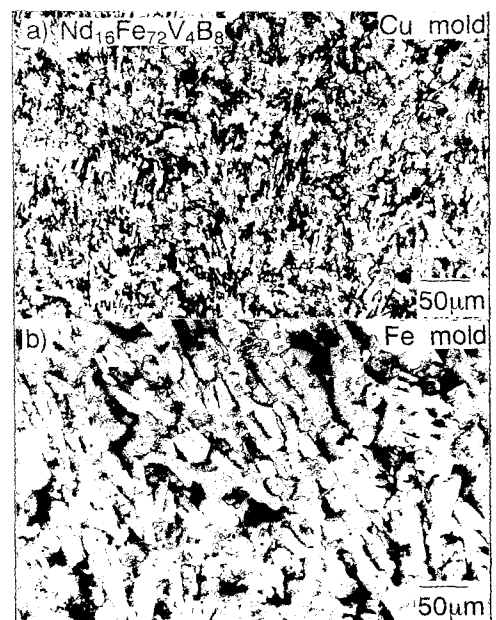


Fig. 2. Optical micrographs of  $\text{Nd}_{16}\text{Fe}_{72}\text{V}_4\text{B}_8$  ingots prepared from (a) copper mold and (b) iron mold.

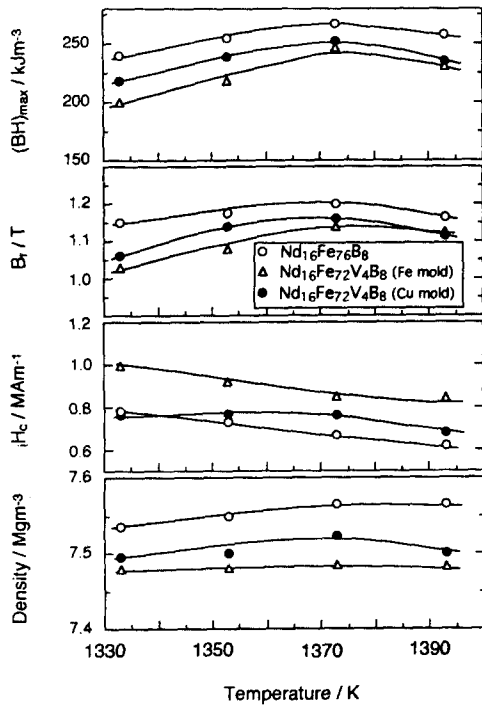


Fig. 3. Magnetic properties of  $\text{Nd}_{16}\text{Fe}_{6-x}\text{V}_x\text{B}_8$  as a function of sintering temperature ( $x=0, 4$ )

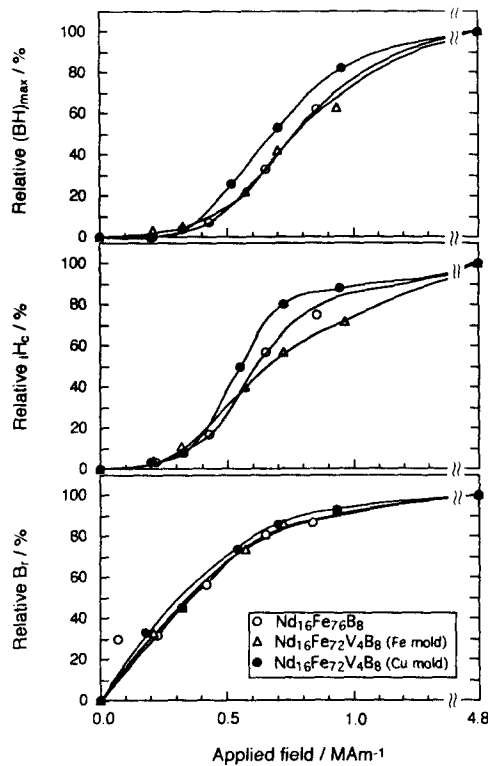


Fig. 4. Relative  $(BH)_{max}$ ,  $iH_c$  and  $B_r$  of  $\text{Nd}_{16}\text{Fe}_{6-x}\text{V}_x\text{B}_8$  as a function of applied field ( $x=0, 4$ ).

$=0, 4$ ) sintered magnets.  $\text{Nd}_{16}\text{Fe}_{72}\text{V}_4\text{B}_8$  alloy prepared from copper mold exhibits higher relative  $(BH)_{max}$  and relative coercivity values than either  $\text{Nd}_{16}\text{Fe}_{76}\text{B}_8$  and  $\text{Nd}_{16}\text{Fe}_{72}\text{V}_4\text{B}_8$  alloys prepared from

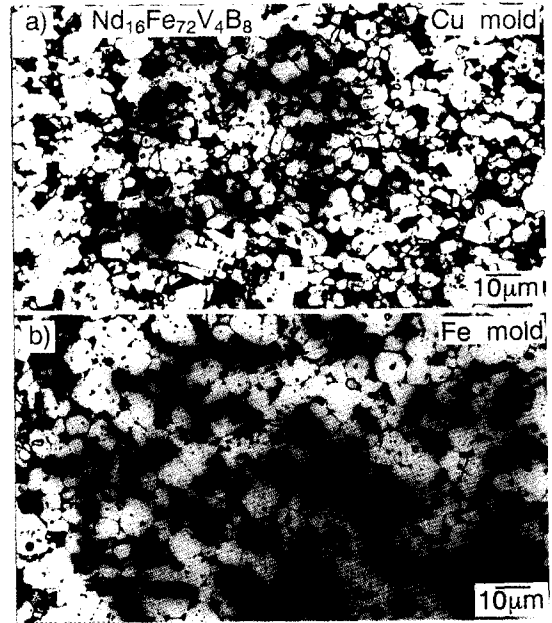


Fig. 5. Optical micrographs of  $\text{Nd}_{16}\text{Fe}_{72}\text{V}_4\text{B}_8$  sintered magnets prepared from (a) copper mold, and (b) iron mold.

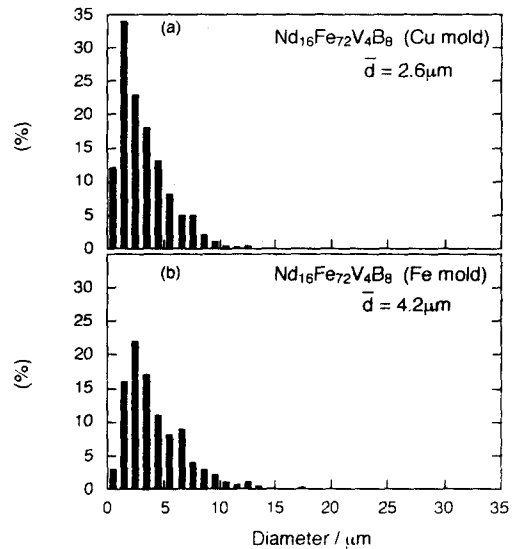


Fig. 6. Grain size distribution of  $\text{Nd}_{16}\text{Fe}_{72}\text{V}_4\text{B}_8$  sintered magnets (a) copper mold and (b) iron mold.

iron mold, but the relative  $B_r$  values appear to be the same for these alloys.

Figure 5 shows optical micrographs for  $\text{Nd}_{16}\text{Fe}_{72}\text{V}_4\text{B}_8$  sintered magnets prepared from copper and iron molds. The alloy prepared from the copper mold has a finer grain size than the alloy from the iron mold. The corresponding grain size distributions are shown in figure 6. The  $\text{Nd}_{16}\text{Fe}_{72}\text{V}_4\text{B}_8$  alloy prepared from the copper mold contains many small grains less than  $5\mu\text{m}$  in diameter and has a narrower grain size distribution. The iron mold alloy shows a

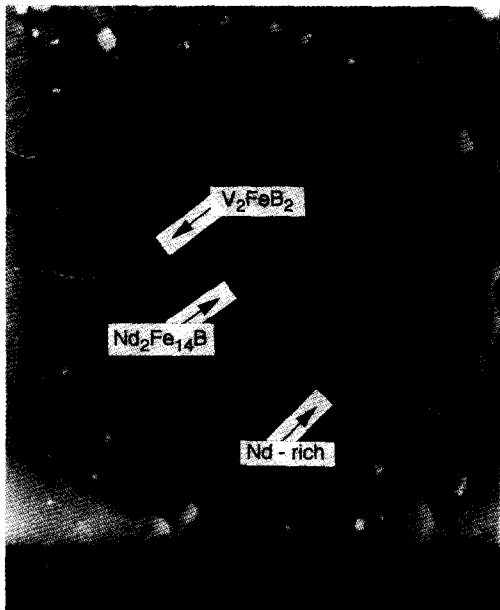


Fig. 7. Microstructure of Nd<sub>16</sub>Fe<sub>72</sub>V<sub>4</sub>B<sub>8</sub> sintered magnets.

broad grain size distribution and contains relative large grains more than 10 $\mu$ m in diameter.

Kronmüller et al. reported that a strong local demagnetization field will be eliminated by suppressing precipitation of the nonmagnetic phase and by reducing the average grain size.<sup>12,13</sup> Hirosawa et al.<sup>10</sup> reported magnetizing ability increases with a decrease in grain size because of a decrease in the strength of the local demagnetization field. When a copper mold is used the casting cooling rate is

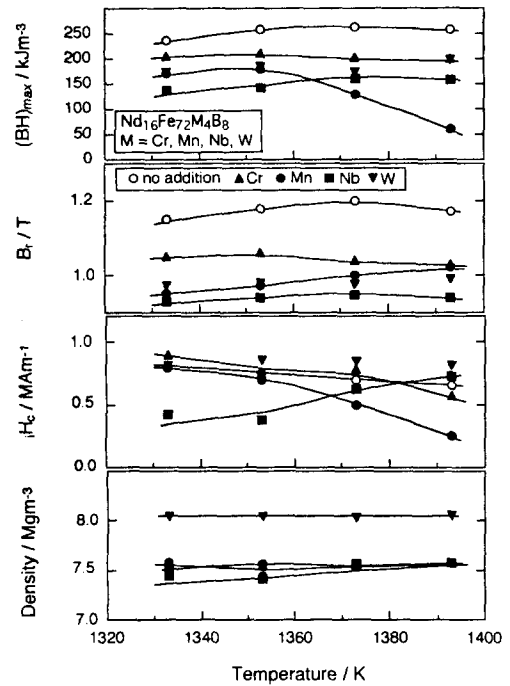


Fig. 8. Magnetic properties of Nd<sub>16</sub>Fe<sub>72-x</sub>V<sub>x</sub>B<sub>8</sub> as a function of sintering temperature (M=Cr, Mn, Nb, W x=0, 4).

higher and finer dispersive borides can form. These borides as show in figure 7 probably work as inhibitors of grain growth during sintering. This result in a narrower grain size distribution and, consequently, a good magnetizing ability can be obtained.

Figure 8 shows the variation in magnetic properties of Nd<sub>16</sub>Fe<sub>72</sub>M<sub>4</sub>B<sub>8</sub> (M=Cr, Mn, Nb and W)

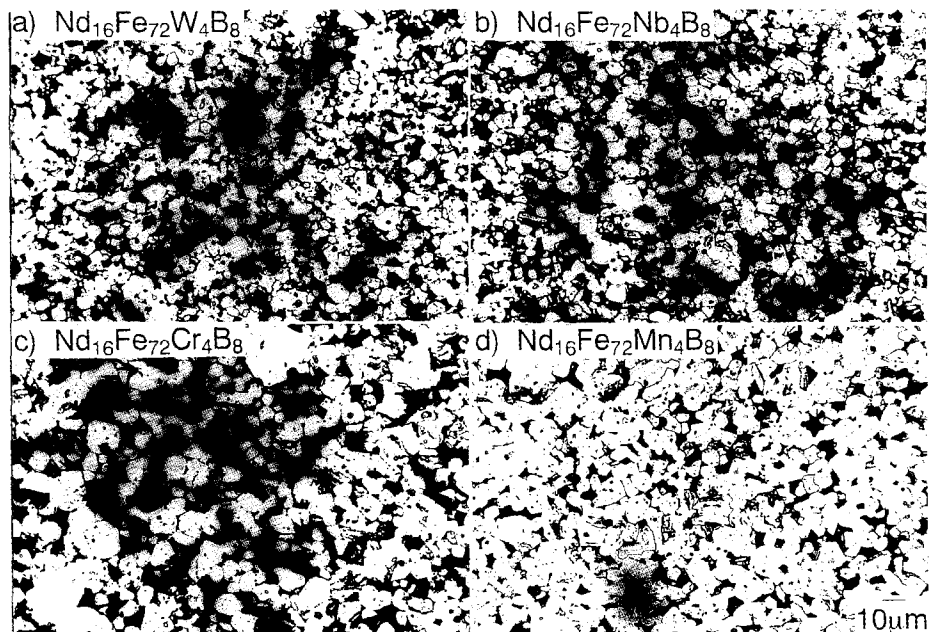


Fig. 9. Optical micrographs of Nd<sub>16</sub>Fe<sub>72-x</sub>V<sub>x</sub>B<sub>8</sub> sintered magnets (M=Cr, Mn, Nb, W x=4).

alloys vs. sintering temperatures in comparison with  $Nd_{16}Fe_{76}B_8$  alloys. The addition of W, a relatively heavy element, results in a high density magnet. The density of Nb containing magnets increases with increasing temperature in comparison with other magnets. Cr containing magnets show a high remanence compared with magnets containing other added elements. All sintered magnets have lower  $(BH)_{max}$  values than do  $Nd_{16}Fe_{76}B_8$  magnets because of decreased remanence. However, Cr and W containing magnets have a higher coercivity than do  $Nd_{16}Fe_{76}B_8$  magnets.

The  $Nd_{16}Fe_{72}Cr_4B_8$  alloy sintered at 1333K shows the highest coercivity value of 0.96MA/m. Figure 9 shows optical micrographs of  $Nd_{16}Fe_{76-x}M_xB_8$  ( $M = Cr, Mn, Nb, W, X=4$ ) sintered magnets. W or Nb containing alloys have a finer microstructure than Cr or Mn containing alloys. Addition of either W or Nb to an alloy inhibits grain growth during sintering, but Cr and Mn additions do not cause this type of inhibition.

Figure 10 shows the relative magnetic properties of Cr, W and V containing alloys in comparison with the properties of  $Nd_{16}Fe_{76}B_8$  alloy. The relative  $(BH)_{max}$  value of an alloy containing Cr is almost equal to the value of  $Nd_{16}Fe_{72}V_4B_8$  alloy. Alloys

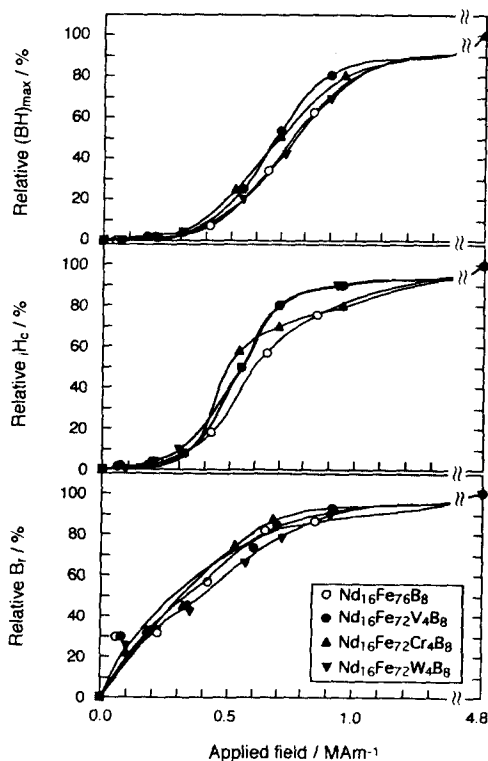


Fig. 10. Relative  $(BH)_{max}$ ,  $H_c$  and  $B_r$  of  $Nd_{16}Fe_{76-x}M_xB_8$  as a function of applied field ( $M = Cr, V, W, x = 0, 4$ ).

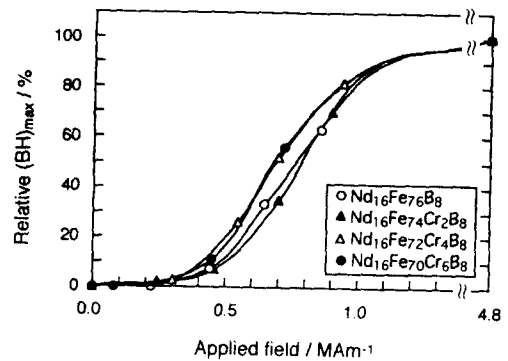


Fig. 11. Relative  $(BH)_{max}$ , of  $Nd_{16}Fe_{76-x}Cr_xB_8$  as a function of applied field ( $x = 0, 2, 4, 6$ ).

containing W show  $H_c$  values which are almost equal to  $Nd_{16}Fe_{72}V_4B_8$  alloys. The relative  $(BH)_{max}$  value of  $Nd_{16}Fe_{72}Cr_4B_8$  alloy is higher than the value for  $Nd_{16}Fe_{76}B_8$  alloy by approximately 10% at 0.96MA/m. However, figure 11 does not show any dependence of relative  $(BH)_{max}$  values on Cr content. Microstructural analysis reveals that sintered magnets with added Cr have relatively large grains with a grain size distribution that is not especially narrow. Inhibition of grain growth by the formation of borides does not occur in Cr containing alloys. Further research will be required to understand why grain growth is not inhibited yet a magnetizing ability is obtained in alloys with added Cr.

#### 4. Conclusions

The alloy prepared from the copper mold has a finer grain size than the alloy from the iron mold. At applied field of 0.8MA/m,  $Nd_{16}Fe_{72}V_4B_8$  magnet prepared from copper mold exhibits about 20% higher relative  $(BH)_{max}$  and about 25% higher relative coercivity values than either  $Nd_{16}Fe_{76}B_8$  and  $Nd_{16}Fe_{72}V_4B_8$  magnets prepared from iron mold, but the relative  $B_r$  values appear to be the same for these alloys. The relative  $(BH)_{max}$  value of  $Nd_{16}Fe_{72}Cr_4B_8$  alloy is higher than the value for  $Nd_{16}Fe_{76}B_8$  alloy by approximately 10% at 0.96MA/m. Microstructural analysis reveals that sintered magnets with added Cr have relatively large grains with a grain size distribution that is not especially narrow.

#### 5. Acknowledgement

The authors would like to thank to Mr. Shintani for his helpful assistance in preparing or measuring samples.

## References

1. J.J. Croat, J.F. Herbst, R.W. Lee and F.E. Pinkerton : J. Appl. Phys., **55**, 2078 (1984)
2. M. Sagawa, S. Fujimura, M. Togawa, H. Yamamoto and Y. Matsuura : J. Appl. Phys., **55**, 2083 (1984)
3. A.J. Williams, P.J. McGuinness and I.R. Harris : J. Less-Common Met **171**, 149 (1991)
4. M. Tokunaga, H. Kogure, M. Endoh, and H. Harada : IEEE Trans. Mag. **23**, 2287 (1987)
5. E. Otsuki, T. Otsuka and T. Imai : in Proc. of the 11th Int. Workshop on Rare Earth Magnets and Their Applications, Pittsburgh, **1**, 328 (1990)
6. M. Sagawa, S. Fujimura, H. Yamamoto, Y. Matsuura and K. Hiraga : IEEE Trans. Mag. **20**, 1584 (1984)
7. J. Hu, Z. Wang, Y. Wang, J. Zhao, X. Rao and N. Zhang : IEEE Trans. Mag. **25**, 3429 (1989)
8. S. Hirosawa, H. Tomizawa, S. Mino and K. Tokuhara : J. Mag. Soc. Japan, **15**, 245 (1991)
9. M. Sagawa, P. Tenaud, F. Vial, K. Hiraga : IEEE Trans. Mag. **26**, 1957 (1990)
10. H. Kanekiyo, S. Mino and S. Hirosawa : J. Mag. Soc. Japan, **16**, 143 (1992)
11. S. Hirosawa, H. Tomizawa, S. Mino and A. Hamamura : IEEE Trans. Mag. **26**, 1960 (1990)
12. G. Martinek and H. Kronmüller : J. Magn. Magn. Mat. **86**, 177 (1990)
13. . Pastushenkov, K. -D. Durst, H. Kronmüller : Phys. Stat. Sol. (a)**104**, 487(1987)